

1752. A contrast between classical method and finite element method for calculating strength in impeller of centrifugal pump

Yan Wang¹, Baode Jing², Chunfu Gao³

Zhejiang Normal University, Jinhua, Zhejiang, 321004, China

²Corresponding author

E-mail: ¹1554200861@qq.com, ²younger9435@126.com, ³cfgao2003@zjnu.cn

(Received 8 May 2015; received in revised form 28 July 2015; accepted 11 August 2015)

Abstract. In order to calculate accurately the stress and the deformation conditions of the closed impeller of centrifugal pumps in the flow field, “direct-calculation method” and the ANSYS Workbench-based finite element method are separately used to calculate the maximum stress that the impeller bears and the strength check of it have been proceed. This paper has made a comparative analysis between the two methods, and it is shown that the finite element analysis method can more comprehensively show the stress concentration, whereas the traditional method is more focused on the average of checking. Therefore, in terms of the results, it is suggested that in addition to the traditional direct-calculation method, modern simulation software such as the finite element method should be used for the proofread of the impeller in the industry, in order to improve the running safety and the reliability of the closed impeller of centrifugal pumps.

Keywords: impeller, strength, finite element method (FEM), direct-calculation method.

1. Introduction

Nowadays, the approximation methods [1-3] are generally adopted to calculate the strength of the centrifugal pump impeller. However, these methods can only roughly estimate the stress of the impeller [4], but not the stress characteristics of the precise position and the maximum stress position. Moreover, the finite element method is also adopted to perform strength calculation, but without consideration of the impact the solid movement deformation posed to the flow field, one-way coupling method leads to calculation errors. Thus, this paper use both “direct-calculation method” [5] and “the finite element method” [6] to calculate the strength of the centrifugal pump impeller. For “direct-calculation method”, it’s combined with MATLAB software to calculate the strength of the impeller’s main wheel and the side wheel. With the two-way coupling in the finite element analysis software-ANSYS, the strength of the centrifugal pump impeller rotating with the motor while buffeting by water can be fully embodied. Moreover, the impeller strength obtained by both methods meets the requirements.

2. Direct-calculation method [5]

A centrifugal pump impeller whose main wheel and side wheel are both round plates with equivalent thickness is made of cast aluminum alloy; its brand is of YL108; its elongation delta is $\delta = 1\%$; its elastic modulus is $E = 70 \text{ GPa}$; its Poisson’s ratio is $\mu = 0.3$, $\sigma_s = 280 \text{ MPa}$ and $\sigma_B = 310 \text{ MPa}$, and its density is $\rho = 2.77 \text{ g/cm}^3$ [7]. Generally, in engineering, those materials whose elongation delta δ is smaller than 5 % are referred to as brittle materials. Thus, the strength of the impeller is to be checked according to the method of brittle material [8]. The main dimensions are shown in Fig. 1, and the maximum speed is $n = 60 \text{ r/s}$, and the number of vane is $Z = 7$.

1) Divide the main wheel and the side wheel into seven segments; record the original data, which is shown in Fig. 1, where r_i ($i = 1, \dots, 8$) is used to represent each radius of 7 segments from the main wheel, which is shown in Table 1, R_i ($i = 1, \dots, 8$) is used to represent each radius of 7 segments from the side wheel, which is shown in Table 2, $h(n)$ is the thickness of the main

wheel at radius r or the thickness of the side wheel at radius R , $h(\pi) = 3.5$ mm is the thickness of blade, $b = 2.5$ mm is the width of blade, $\beta = 70^\circ$ is the angle between the tangent and the diameter of the blade.

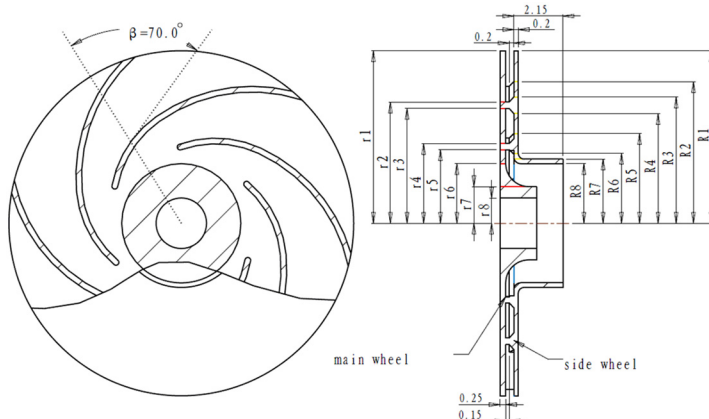


Fig. 1. The impeller

2) Determine the additional load value on the vane with the Eq. (1), and 50 % of the vane weight is born by the main wheel while 30 % of the vane weight is born by the side wheel, whereas the remaining 20 % of the load is compensated by the shear stress in the blade cross section:

$$\rho_{np} = \rho \left[1 + \frac{zb_\pi h_\pi}{2\pi rh_n \cos\beta} \right]. \quad (1)$$

3) Determine the value of σ_t and σ_r with Eqs. (2), (3) and (4).

$$\begin{cases} \sigma_t = \frac{C_1 E}{1 - \mu} + \frac{C_2 E}{(1 + \mu)r^2} - \frac{1 + 3\mu}{8} \rho \omega^2 r^2, \\ \sigma_r = \frac{C_1 E}{1 - \mu} - \frac{C_2 E}{(1 + \mu)r^2} - \frac{3 + \mu}{8} \rho \omega^2 r^2. \end{cases} \quad (2)$$

The boundary conditions in the outer contour of the impeller (the first loop) are as follows.

When $r = r_1$, $\sigma_r = 0$, and $\sigma_t = \sigma_0$, where σ_0 is the unknown hoop stress.

Determine the constant C_1 with the Eq. (2) and the constant C_2 according to the boundary conditions. Then, substitute C_1 and C_2 into the Eq. (2). It is defined that $A = \sigma_t + \sigma_r$, $B = \sigma_t - \sigma_r$. For the first loop, that is, at $r = r_2$, it has:

$$\begin{cases} A_I = \sigma_0 + \frac{1 + \mu}{2} \rho \omega^2 r_1^2 \left[1 - \left(\frac{r_2}{r_1} \right)^2 \right], \\ B_I = \sigma_0 \left(\frac{r_1}{r_2} \right)^2 - \frac{1 - \mu}{4} \rho \omega^2 r_1^2 \left[\left(\frac{r_1}{r_2} \right)^2 - \left(\frac{r_2}{r_1} \right)^2 \right]. \end{cases} \quad (3)$$

The stress of the first loop at r_2 is:

$$\begin{cases} \sigma_{tI} = \frac{A_I + B_I}{2}, \\ \sigma_{rI} = \frac{A_I - B_I}{2}. \end{cases} \quad (4)$$

When $r = r_6$, the thickness between the adjacent loops mutates. In order to determine the stress of the sixth loop at r_6 , it can be obtained by the consistency condition that:

$$\sigma_{rVI} = \frac{h_{nV}}{h_{nVI}} \sigma_{rV}, \quad \sigma_{tVI} = \mu \Delta \sigma_r + \sigma_{tV}, \quad \Delta \sigma_r = \sigma_{rVI} - \sigma_{rV}. \quad (5)$$

Table 1. The stress calculation in each segment of the main wheel

Segment number	Main wheel						
	r	r^2	$h(n)$	$dV(n) = 2\pi rh(n)dr$	$dV(\pi) = \frac{zbh(n)}{\cos\beta} dr$		
1	7.525	56.626	0.250	22.525		4.012	
2	5.285	27.931	0.250	2.238		0.496	
3	5.008	25.080	0.250	10.219		2.749	
4	3.473	12.062	0.250	1.385		0.473	
5	3.209	10.298	0.250	2.777		1.091	
6	2.600	6.760	0.250	12.543		1.791	
7	1.600	2.560	1.600	6.782		0.000	
8	1.100	1.210	1.600	—		—	
	$\rho np = \rho \frac{dV(n) + dV(\pi)}{dV(n)}$	$\rho np' = k\rho \frac{dV(n) + dV(\pi)}{dV(n)}$		A (MPa)	B (MPa)	σ_{tmain} (MPa)	σ_r (MPa)
1	0.000326	0.000302		14.814	14.814	14.814	0.000
2	0.000338	0.000308		35.070	13.524	24.297	10.773
3	0.000352	0.000314		37.527	13.525	25.526	12.001
4	0.000372	0.000324		47.585	19.304	33.444	14.140
5	0.000386	0.000331		49.969	19.950	34.960	15.010
6	0.000317	0.000297		53.483	26.473	39.978	13.505
7	0.000277	0.000277		48.423	6.893	27.658	20.765
8	—	—		46.797	46.797	46.797	0.000

Table 2. The stress calculation in each segment of the side wheel

Segment number	Side wheel						
	R	R^2	$h(n)$	$dV(n) = 2\pi Rh(n)dR$	$dV(\pi) = \frac{zbh(n)}{\cos\beta} dR$		
1	7.525	56.626	0.200	11.630		0.000	
2	6.173	38.106	0.200	4.899		0.547	
3	5.505	30.305	0.200	4.647		0.589	
4	4.786	22.906	0.200	4.759		0.713	
5	3.915	15.327	0.200	3.784		0.708	
6	3.050	9.303	0.200	0.999		0.205	
7	2.800	7.840	2.150	6.562		0.000	
8	2.600	6.760	2.150	—		—	
	$\rho np = \rho \frac{dV(n) + dV(\pi)}{dV(n)}$	$\rho np' = k\rho \frac{dV(n) + dV(\pi)}{dV(n)}$		A (MPa)	B (MPa)	σ_{tmain} (MPa)	σ_r (MPa)
1	0.000277	0.000277		17.355	17.355	17.355	0.000
2	0.000308	0.000286		29.359	17.755	23.557	5.802
3	0.000312	0.000288		34.987	18.811	26.899	8.088
4	0.000319	0.000289		40.042	21.695	30.869	9.173
5	0.000329	0.000293		45.327	28.763	37.045	8.282
6	0.000334	0.000294		49.751	43.827	46.789	2.962
7	0.000277	0.000277		49.008	37.235	43.121	5.887
8	—	—		47.765	47.765	47.765	—

As the impeller is loosely slipped over rather than an interference fit on the shaft, therefore, at the inner contour of r_8 , it has $\sigma_r = 0$. Based on the boundary conditions, σ_0 is determined by

MATLAB. Then substitute σ_0 to the stress expression and then the stress of each loop is obtained. Further, it's shown graphically in Table 1 and Table 2.

4) Draw the stress image according to the data in Fig. 1, as shown in Fig. 2.

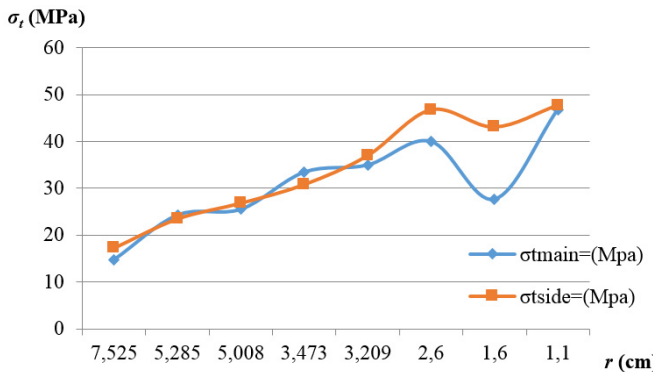


Fig. 2. The stress image of the main wheel and the side wheel of the impeller

5) Check the strength of the brittle material impeller.

The strength condition of the brittle material impeller is $\sigma_{\max} \leq [\sigma]$ here $[\sigma] = \varepsilon \sigma_B / n_B$, and the impact factor of the absolute size (thickness) $\varepsilon = 0.74$, and the safety factor of strength $n_B = 4$.

Thus, it can be calculated that $[\sigma] = 57.35$ MPa; the maximum stress of the main wheel $\sigma_{\max\text{main}} = 46.7965$ MPa; the maximum stress of the side wheel $\sigma_{\max\text{side}} = 47.765$ MPa, all satisfying the strength condition.

3. The finite element method

In this paper, the large general finite element software-ANSYS Workbench is adopted to analyze the fluid structure coupling of impeller and water [9, 10]. First, analyze the flow field with ANSYS CFX and get the water pressure on the impeller. Then, substitute the data to the statics analysis module and determine the stress and deformation of the impeller. Finally, substitute the data to modal analysis and obtain the first eight modes of the impeller [11].

3.1. The establishment of a 3D model and the extraction of the flow channel

As shown in Fig. 3, the 3D model of impeller is established by the 3D drawing software-CREO 2.0. Then, it is imported into ANSYS workbench to create a Geometry, and after that the flow channel is extracted utilizing the command “fill” in the Design Modeler, as shown in Fig. 4.

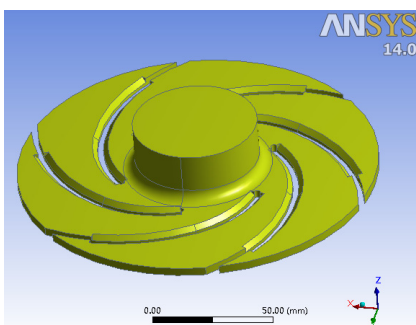


Fig. 3. The impeller

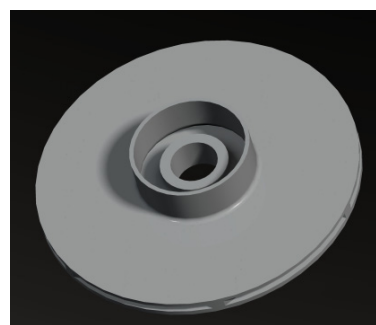


Fig. 4. The flow channel

3.2. Fluid-structure coupling of the impeller

Fluid-structure interaction analysis of the impeller was conducted through ANSYS Workbench, and the process is shown in Fig. 5 [12].

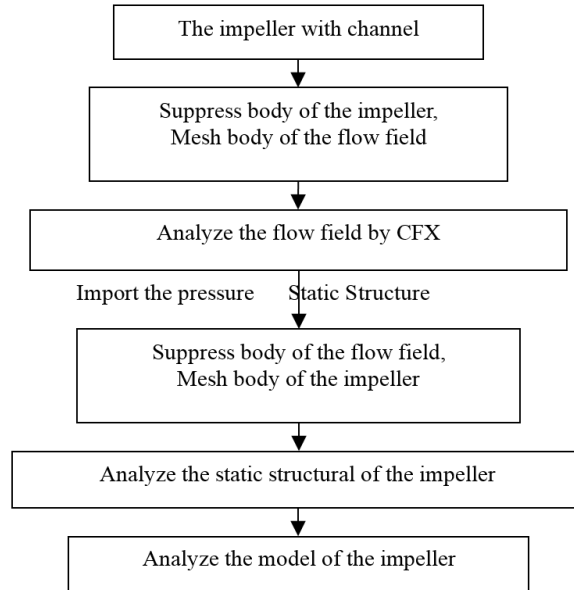


Fig. 5. Flow chart

3.2.1. The flow field analysis

When analyzing the flow field, suppress body of the impeller first. Then, the body of the flow field is meshed with the element size of 2 mm, and the main surface of the flow field is set as boundary of 3 layers. Based on the tetrahedral meshing method, the flow field is meshed to 173579 elements in total, the mesh diagram of the flow field is shown in Fig. 6 and the inflation of it is shown in Fig. 7.

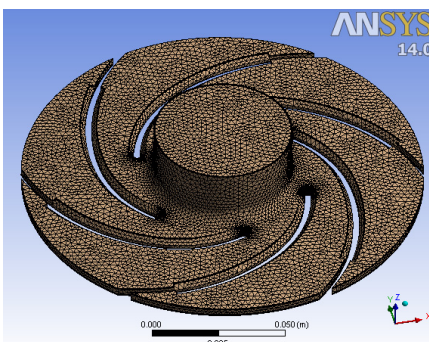


Fig. 6. The meshing diagram of the flow

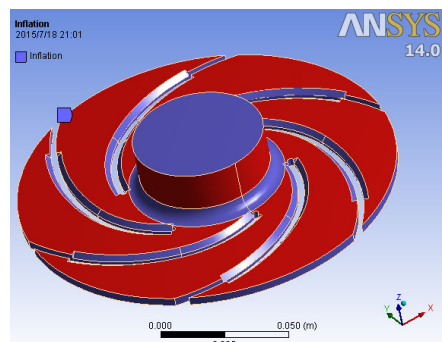


Fig. 7. The inflation of the impeller

Then, define the boundary condition of the inflow-port and the outflow-port as “inlet” and “outlet”, respectively, whereas the normal speed is 2.65 m/s and the relative pressure is 1 atmosphere. Moreover, define the boundary condition of all the surfaces except inflow-port and outflow-port as “wall”, as shown in Fig. 8. After that, start running until the solutions are

convergent. From the velocity streamline of the flow field (Fig. 9), it can be seen that the flow velocity on the pressure surface increases gradually with the increasing of the radius, and reaches the maximum near the inflow-port. Meanwhile, from the pressure figure of the flow field (Fig. 10), it can be seen that the maximum pressure is in the inflow-port of the impeller, and decreases with the water being thrown away by the centrifugal force.

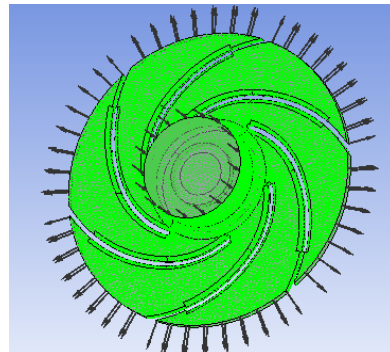


Fig. 8. Define the boundary condition of the flow field

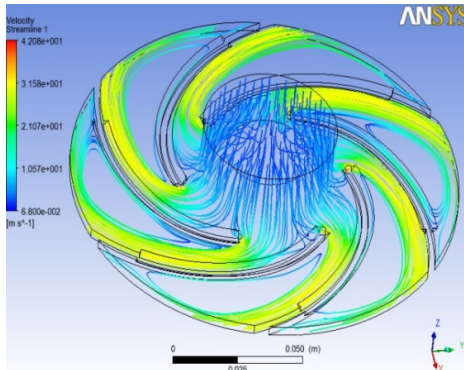


Fig. 9. The velocity streamline of the flow field

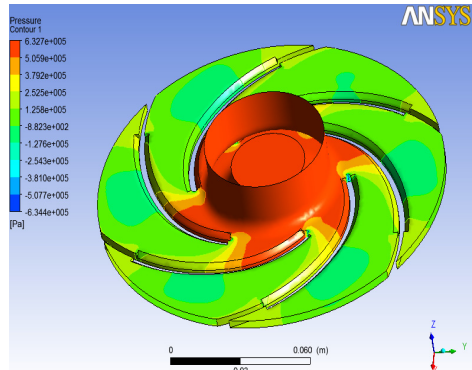


Fig. 10. The pressure figure of the flow field

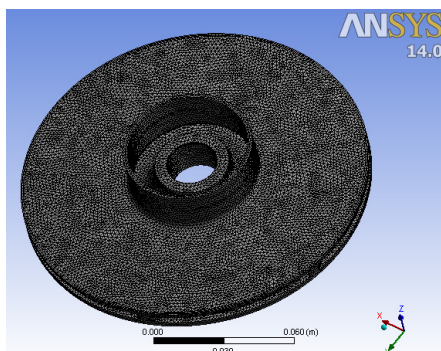


Fig. 11. The meshing diagram of the impeller

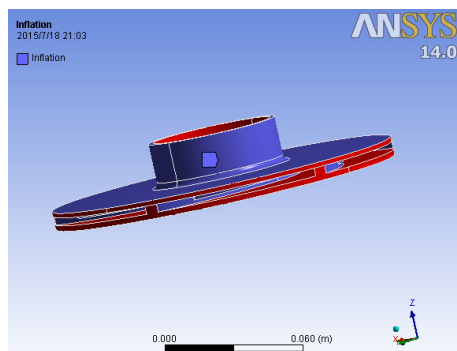


Fig. 12. The inflation of the impeller

3.2.2. Impeller structure statics analysis

In engineering materials database of ANSYS Workbench, aluminum alloy is selected to suppress body of the flow field except the solid impeller. Then, the body of the impeller is meshed with the element size of 1.5 mm, and the main surface of the impeller is set as boundary of 3 layers.

Based on the automatic meshing method, the impeller is meshed to 255439 elements in total. The mesh diagram of the impeller is shown in Fig. 11 and the inflation of it is shown in Fig. 12.

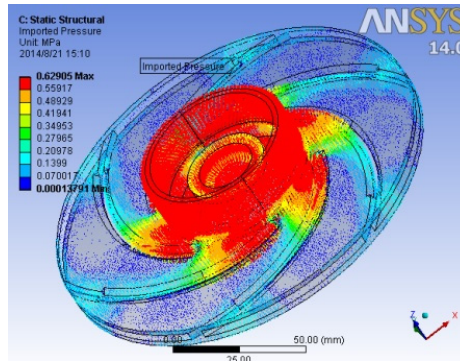


Fig. 13. The imported impeller pressure

The solution of the fluid flow (CFX) is imported to the Static Structure, with the imported impeller pressure as shown in Fig. 13. Then, define the rotation velocity on the center axis of the impeller as 60 r/s, and add a fixed support on the inflow-surface to solve the structural statics.

The results of the finite element analysis are shown in Fig. 14, and the maximum stress and the total deformation of the impeller can be known from it. It can be seen that the maximum total deformation of 1.6948 e-002 mm appears in the outside diameter of the main impeller, as marked in the figure. According to the fourth strength theory, the maximum equivalent stress is 24.99 MPa, which appears in the tail-end blade, as marked in the figure [13].

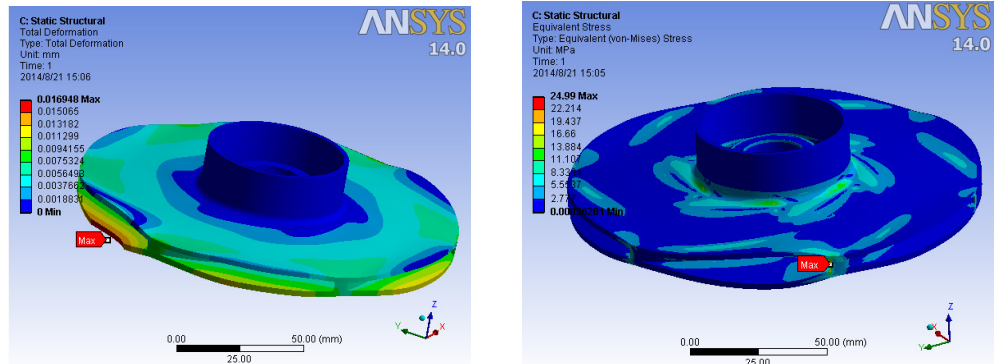


Fig. 14. Results of the finite element analysis

3.2.3. Impeller modal analysis

Modal analysis is a very effective method to avoid the potential resonance of the impeller. Without considering gravity, the modal analysis of hydraulic loading and rotation is conducted with the final data of fluid-solid coupling being introduced. Moreover, the first eight order modes of impeller and its corresponding frequency are shown in Fig. 15. Meanwhile, it is shown in Table 3 the results of the impeller modal analysis of the flow field.

Table 3. The results of the impeller modal analysis in the flow field (Hz)

Mode	1	2	3	4	5	6	7	8
Frequency	1705.9	1706	2043.5	2245.4	2245.5	3233.9	4010.7	5071.1

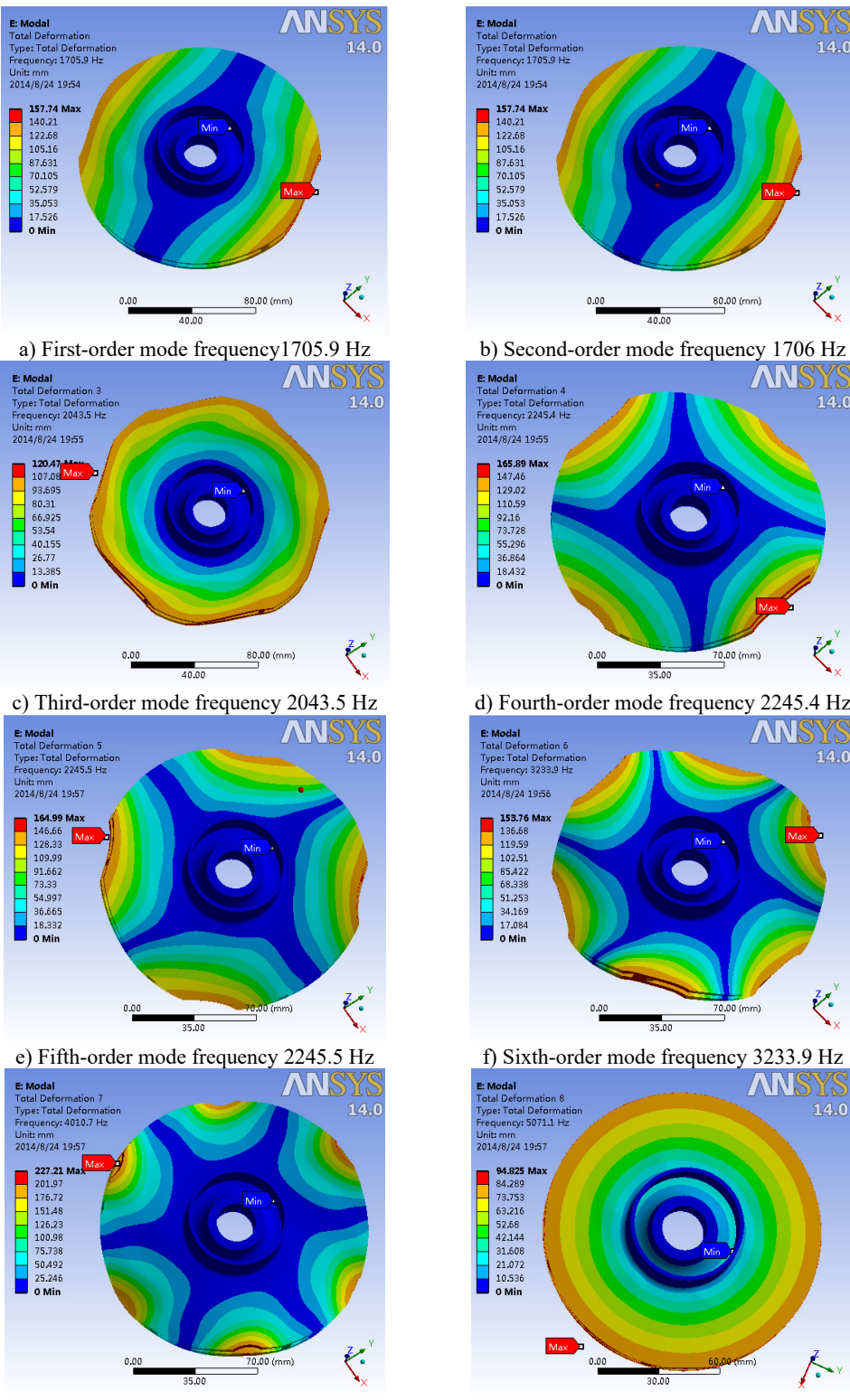


Fig. 15. The first eight order modal of the impeller and the corresponding frequency

4. Conclusion

The maximum stress calculated by the fluid-structure coupling to impeller and the flow field is less than that obtained by the “once calculation method”. The method of fluid-structure coupling concerns about the pressure of the fluid flow on the impeller while combining with the structure statics by using the two-way coupling to get the final stress. However, for the traditional “once calculation method”, only the structure statics is used and only the average stress is considered which can hardly know the stress concentration source. Even if it is considered that the plastic deformation of the stress concentration areas is intensified, the strength checking of these areas still cannot be slackened. Thus, based on the comparison between the results of the two methods, it's more comprehensive and reliable to utilize the finite element method. Therefore, it is demonstrated that in the practical production design and checking, more rigorous and efficient data and higher safe reliability of the impeller operation can be realized by combining the conventional computation method with the finite element method.

Acknowledgements

This work was financially supported by The 2014 Scientific and Technological Innovation Activities Plan for University Students in Zhejiang Province (2014R404033) and The National Natural Science Foundation of China (51275483).

References

- [1] **Li Yaofeng, Liu Chuanshao, Zhao Bo** The feasibility theoretical analysis of the pump engineering ceramics impeller. Journal of Henan Polytechnic University: Natural Science Edition, Vol. 25, Issue 4, 2006, p. 313-317, (in Chinese).
- [2] **Ma Xinhua, Sang Jianguo, Li Juan** Strength calculation for plastic pump impeller. Drainage and Irrigation Machinery, Vol. 25, Issue 2, 2007, p. 23-25, (in Chinese).
- [3] **Kong Fanyu, Liu Jianrui, Shi Weidong** Calculation of axial force balance for high-speed magnetic drive pump. Transactions of the Chinese Society of Agricultural Engineering, Vol. 21, Issue 7, 2005, p. 69-72, (in Chinese).
- [4] **Wang Yang, Wang Hongyu, Zhang Xiang** Strength analysis on the stamping and welding impeller in centrifugal pump based on fluid-structure interaction theorem. Transactions of the Chinese Society of Agricultural Engineering, Vol. 27, Issue 3, 2011, p. 131-136, (in Chinese).
- [5] **Guan Xingfan, Yao Zhaosheng** Strength Calculation of Pump Parts. China Machine Press, 1981, p. 91-97, (in Chinese).
- [6] **Liu Houlin, Xu Huan, Wu Xianfang** Effect of fluid-structure interaction on internal and external characteristics of centrifugal pump. Transactions of the Chinese Society of Agricultural Engineering, Vol. 28, Issue 13, 2012, p. 82-87, (in Chinese).
- [7] **Cheng Daxian** Handbook of Mechanical Design. Chemical Industry Press, 2007, (in Chinese).
- [8] **Liu Hongwen** Mechanics of Materials. Higher Education Press, Beijing, 2011, (in Chinese).
- [9] ANSYS CFX. Release 12.0, USA, 2009.
- [10] **Li Pengfei, Xu Minyi, Wang Feifei** Fluent Gambit ICEM CFD Tecplot. Posts and Telecom Press, 2011, (in Chinese).
- [11] **Zhou Haidong, Zhang Yanwei, Wang Bochao, Pang Wei** Fluid-solid coupling analysis of wind turbine blade based on ANSYS workbench. Hebei Journal of Industrial Science and Technology, Vol. 30, Issue 5, 2013, (in Chinese).
- [12] **Pu Guangyi** ANSYS Workbench 12 Foundation Course and Examples. China Water Power Press, 2010, (in Chinese).
- [13] **Cai Jiancheng, Yuan Minjian, Lu Fu'an, Qi Datong, Qiu Chang'an** A contrast between classical method and finite element method for calculating strength of impeller parts in centrifugal fans. Compressor Blower and Fan Technology, Vol. 5, 2007, p. 30-33, (in Chinese).



Yan Wang is studying in Zhejiang Normal University, Jinhua, China. Her current research interests include hydraulic transmission and control.



Baode Jing received Ph.D. degree in Jilin University, Changchun, China, in 2005. Now he works at Zhejiang Normal University. His current research interests include hydraulic transmission and control.



Chunfu Gao received Ph.D. degree in Jilin University, Changchun, China, in 2000. Now he works at Zhejiang Normal University. His current research interests include electromechanical integration.